

Poor screening and nonadiabatic superconductivity in correlated systemsLilia Boeri,¹ Emmanuele Cappelluti,^{1,2} Claudio Grimaldi,³ and Luciano Pietronero^{1,4}¹*Dipartimento di Fisica, Università "La Sapienza," Piazzale A. Moro 2, 00185 Roma, Italy
and INFM UdR RM1, Roma, Italy*²*"Enrico Fermi" Center, via Panisperna 89a, c/o Compendio del Viminale, 00184 Roma, Italy*³*Institut de Production et Robotique, LPM, École Polytechnique Fédérale de Lausanne, CH-1015 Lausanne, Switzerland*⁴*CNR, Istituto di Acustica "O.M. Corbino," via del Fosso del Cavaliere 100, 00133 Roma, Italy*

(Received 10 July 2003; revised manuscript received 19 September 2003; published 23 December 2003)

In this paper we investigate the role of the electronic correlation on the hole doping dependence of electron-phonon and superconducting properties of cuprates. We introduce a simple analytical expression for the one-particle Green's function in the presence of electronic correlation and we evaluate the reduction of the screening properties as the electronic correlation increases by approaching half filling. The poor screening properties play an important role within the context of the nonadiabatic theory of superconductivity. We show that a consistent inclusion of the reduced screening properties in the nonadiabatic theory can account in a natural way for the T_c - δ phase diagram of cuprates. Experimental evidences are also discussed.

DOI: 10.1103/PhysRevB.68.214514

PACS number(s): 74.20.Mn, 71.10.Hf, 63.20.Kr

I. INTRODUCTION

The role of the electron-phonon (el-ph) interaction in the high- T_c superconducting cuprates has been a matter of debate for a long time. In early times the report of a negligible isotope effect on T_c at optimal doping, the almost linear behavior of the resistivity on temperature, also at optimal doping, and other exotic features of the copper oxides led to the common belief that electron-phonon coupling was a marginal ingredient to understanding the phenomenology of these materials. However, over the years, there has been a revamping evidence of an important role of the phonons. The most remarkable ones are, for instance, the discovery of an isotope effect on T_c larger than the BCS value ($\alpha_{T_c} > 0.5$) in the underdoped regime,^{1,2} the report of a sizable isotope shift on the effective electronic mass m^* (Ref. 3) and on the onset of the pseudogap,^{4,5} and the observation of phonon renormalization⁶ and phonon anomalies at $T < T_c$.⁷ More recently, angle-resolved photoemission spectroscopy (ARPES) measurements pointed out a kink in the electron dispersion, the origin of which is probably phononic.⁸ Clearly, if phonons are relevant for superconductivity in these materials, this cannot be described in a BCS-like framework, but some nonconventional approach including strong electronic correlation is necessary. The study of the interplay between electron-phonon interaction and the electronic correlation is a challenging task which has attracted much scientific work along different lines.

An interesting issue concerns the momentum modulation of the electron-phonon coupling induced by the electronic correlation. In Ref. 9, using a variety of theoretical and experimental findings, it is shown that in correlated systems small- \mathbf{q} scattering in the electron-phonon interaction is strongly favored. A strong enhancement of the forward scattering at $\mathbf{q} \sim 0$ in correlated systems close to the metal-insulator transition, accompanied by a suppression of scattering at large \mathbf{q} , was reported, for example, in Refs. 10,11 by using $1/N$ expansion techniques. A recent numerical work

based on quantum Monte Carlo technique confirms this picture.¹²

Different but somehow complementary arguments based on poor screening effects in correlated systems have been also discussed in literature. The basic idea is that as a metal loses its coherence as a function of the correlation degree approaching a metal-insulator transition, the screening properties of the bare long-range electron-phonon interaction become less effective resulting in a net predominance of small- \mathbf{q} scattering.^{13-16,22} A similar physical argument applies, for example, to doped semiconductors which are commonly described in terms of the Fröhlich Hamiltonian, with electron-phonon matrix elements $|g_{\mathbf{q}}|^2 \propto 1/|\mathbf{q}|^2$.

The momentum structure of the electron-phonon scattering induced by the electronic correlation has been shown to play a crucial role in the context of nonadiabatic superconductivity.¹⁷⁻¹⁹ In narrow-band systems, such as cuprates and fullerenes, the Fermi energy E_F is so small as to be comparable with the phonon frequencies ω_{ph} , and the adiabatic assumption ($\omega_{\text{ph}} \ll E_F$) breaks down. In this context Migdal's theorem²⁰ does not apply and one needs to take into account nonadiabatic effects not included in the Migdal-Eliashberg (ME) theory of superconductivity. Detailed studies have shown that the nonadiabatic contributions, which are well represented by the vertex function, present a complex momentum-frequency structure, in which small- \mathbf{q} scattering leads to an enhancement of the effective superconducting pairing, while large- \mathbf{q} scattering leads to its reduction.¹⁷⁻¹⁹ The strong \mathbf{q} -modulation of the electron-phonon interaction due to the electronic correlation is thus expected to give rise to a net enhancement of the superconducting pairing.

The purpose of the present paper is twofold. On one hand we wish to quantify the microscopic dependence of the screening properties of a correlated system on relevant quantities such as the electron density of the Hubbard repulsion; in addition we apply the derived screened electron-phonon interaction to evaluate the role of the electronic correlation in the context of the nonadiabatic superconductivity and to derive a qualitative superconducting phase diagram. To this aim we introduce a model for the electronic Green's function of

the system, based on the decomposition of the total spectral function in a coherent, itinerant part, and an incoherent localized background corresponding to the Hubbard subbands. The relative balance between the two parts varies as a function of doping and electronic correlation. This will have important consequences on the electronic screening and hence on the \mathbf{q} -modulation of the effective electron-phonon scattering, as well as on the superconducting properties. We shall show the following.

(1) The coherent excitations dominate the screening properties as well as the superconducting ones.

(2) The loss of coherent spectral weight approaching half filling is thus responsible for the reduction of the screening properties and for the increase of the forward scattering in the electron-phonon interaction.

(3) In the strongly correlated regime the selection of forward scattering gives rise to an enhancement of the effective electron-phonon interaction within the context of the nonadiabatic superconductivity. These effects however compete with the reduction of the quasiparticle spectral weight which is detrimental for superconductivity.

(4) The resulting phase diagram shares many similarities with one of the cuprates. In particular, it shows an overdoped region, where superconductivity is suppressed by negative nonadiabatic effects, an underdoped region, in which superconductivity is destroyed by the loss of coherent spectral weight, and an intermediate region, in which the predominance of small- \mathbf{q} scattering leads to an enhancement of the nonadiabatic el-ph pairing which overcomes the reduction of the coherent spectral weight.

We hereby wish to point out that a complete description of the rich phenomenology of the cuprates is well beyond the aim of the present paper. In particular, we shall not discuss, for reason of simplicity, the symmetry of the gap, which of course is of fundamental importance if one wishes to give a quantitative description of these systems. We would like just to remark on this point that a d -wave symmetry of the superconducting order parameter was shown by many authors to naturally arise in the context of a phonon pairing with a significant predominance of forward scattering.²¹⁻²⁴ The competition between s - and d -wave symmetry in a nonadiabatic electron-phonon system was also studied in Ref. 25. Taking into account explicitly the d -wave symmetry of the gap would not change in a qualitative way the results of the present work.

This paper is organized as follows. In Sec. II we introduce our model Green's function; in Sec. III we derive an effective form for the electron-phonon interaction. In the last section we write and solve the generalized Migdal-Eliashberg equations, in the adiabatic and nonadiabatic limit, and discuss in detail the competition of the different factors which determine the superconducting critical temperature of our system.

II. A MODEL FOR CORRELATED ELECTRON SYSTEMS

As briefly discussed in the Introduction, one of the main aims of the present paper is to investigate how the screening properties are affected by the presence of strong electronic

correlation, and to parametrize these effects in terms of microscopic quantities. In particular, we have in mind a Hubbard-like system where itinerant electrons, with band dispersion $\epsilon_{\mathbf{k}}$ and bandwidth E , interact each other through an onsite Coulomb repulsion U . As we are going to see, a crucial role is played in this context by the transfer of spectral weight as a function of the correlation degree from low-energy coherent states to the high-energy (Hubbard-like) incoherent ones.

In this section we present a simple, minimal model for the electron spectral function which takes into account these main effects and which can thus represent a proper starting point to evaluate screening effects in correlated systems.

All the possible information about the single-particle properties of the system is contained in the one-electron Green's function $G(\mathbf{k}, \omega)$. Without loss of generality we assume that the Green's function G can be split in a coherent and an incoherent contribution:²⁶

$$G(\mathbf{k}, \omega) = G_{\text{coh}}(\mathbf{k}, \omega) + G_{\text{inc}}(\mathbf{k}, \omega), \quad (1)$$

where the coherent part G_{coh} describes the itinerant, quasiparticle-like properties of the electron wave function, while the incoherent part G_{inc} accounts for the incoherent high-energy excitations. Due to its localized nature $G_{\text{inc}}(\mathbf{k}, \omega)$ is only weakly dependent on the momentum quantum number, so that the dependence on \mathbf{k} can be reasonably neglected.

An important quantity which parametrizes the relative balance between coherent and incoherent contributions is the quasiparticle spectral weight Z , which is simply given by

$$\int d\omega \frac{1}{\pi} \text{Im}[G_{\text{coh}}(\mathbf{k}, \omega + i\delta)] = Z, \quad (2)$$

whereas the incoherent part obeys the sum rule

$$\int d\omega \frac{1}{\pi} \text{Im}[G_{\text{inc}}(\mathbf{k}, \omega + i\delta)] = 1 - Z. \quad (3)$$

The quasiparticle spectral weight Z can vary between 0 and 1, the two limits corresponding to the insulating and metallic limit, respectively. It depends on the internal parameters U and δ , where δ is the hole doping ($\delta = 1 - n$) and n the total number of electrons ($n = 1$ half-filled case).

Several techniques have been developed to investigate the Hubbard model.²⁷ Different starting points are employed according to whether main emphasis has to be laid on the coherent (itinerant) or on the incoherent (localized) features. For instance, the so-called Hubbard I approximation,²⁸ which is exact in the atomic limit, is mainly aimed at a schematic representation of the localized states, described by an upper and a lower Hubbard band spaced by an energy gap of width U . On the other hand the Gutzwiller technique²⁹ and the mean-field slave bosons solution³⁰ offer a useful tool to deal with the coherent spectral weight of the electron Green's function: in this case the quasiparticle spectral properties in the presence of strong correlation are described in terms of an effective band of noninteracting fermions with spectral weight Z and bandwidth ZE .

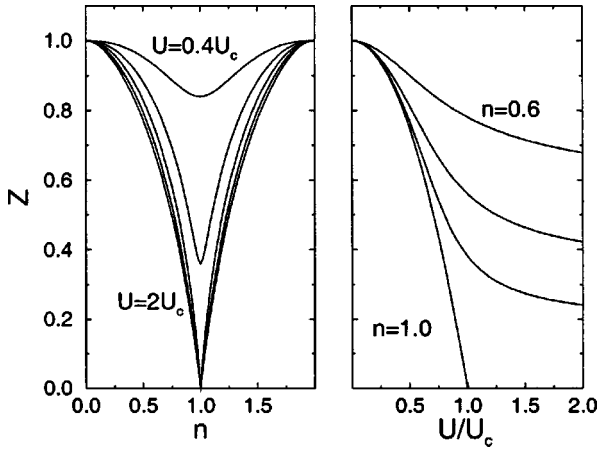


FIG. 1. Quasiparticle spectral weight as determined by the Gutzwiller solution at finite U and n . Left panel: Z as function of n for (from top to the bottom) $U/U_c = 0.4, 0.8, 1.2, 1.6, 2.0$. Right panel: Z as function of U/U_c for (from top to the bottom) $n = 0.6, 0.8, 0.9, 1.0$.

In this paper we introduce a new phenomenological model to take into account in the simplest way and at the same level the coherent and incoherent parts of the Green's function. We approximate the exact (unknown) coherent and incoherent parts of $G(\mathbf{k}, \omega)$ in Eq. (1), respectively, with the Gutzwiller²⁹ and Hubbard I²⁸ solutions

$$G_{\text{coh}}(\mathbf{k}, \omega) = \frac{Z}{\omega - Z\epsilon_{\mathbf{k}} + \mu \pm i0^+}, \quad (4)$$

$$G_{\text{inc}}(\omega) = \frac{(1-Z)}{N_s} \sum_{\mathbf{k}} \left[\frac{(1-n/2)}{\omega - (1-n/2)\epsilon_{\mathbf{k}} + \mu - U/2} + \frac{n/2}{\omega - (n/2)\epsilon_{\mathbf{k}} + \mu + U/2} \right], \quad (5)$$

where μ is the chemical potential, N_s is the total number of sites, and Z is the quasiparticle weight obtained in the Gutzwiller approximation in the paramagnetic state at finite U and generic filling (Appendix A). Due to the localized nature of the incoherent part we have replaced the $G_{\text{inc}}(\mathbf{k}, \omega)$ given by the Hubbard I approximation with its momentum average. Numerical calculations based on dynamical mean-field theory (DMFT) confirm our qualitative picture of a spectral weight transfer from a central coherent peak to an incoherent Hubbard-like background with increasing U .³¹

The behavior of Z as function of the particle density n and of the Hubbard energy U is shown in Fig. 1. The critical Hubbard energy U_c , which determines the Brinkman-Rice transition at $n = 1$ is related to the kinetic energy E_{kin} , which depends on the bare electron dispersion shape, through the relation $U_c = 8|E_{\text{kin}}|$.²⁹ In the following, we employ a bare constant density of states (DOS) with $N(\epsilon_{\mathbf{k}}) = N_0 = 1/E$ for $\epsilon_{\mathbf{k}} \in [-E/2, E/2]$. In this case, we have $U_c = 2E$. The chemical potential μ is determined by the total number of particles. In Fig. 2 we show typical density of states $N(\omega)$ for the correlated system described by our model [Eqs. (4) and (5)].

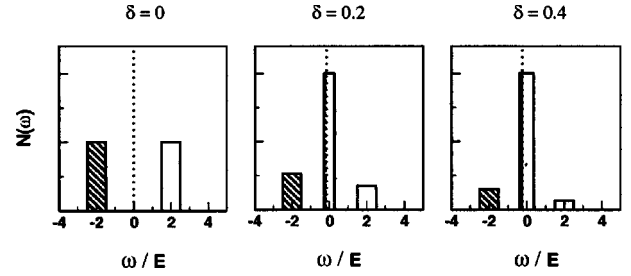


FIG. 2. Density of states $N(\omega) = (1/\pi) \sum_{\mathbf{k}} \text{Im} G(\mathbf{k}, \omega + i0^+)$ resulting from our model, for $U = 2U_c$ and different values of doping. At half filling the system is an insulator, and its density of states is represented by two Hubbard-like features at distance U from each other; moving away from half filling a coherent peak starts forming, with increasing weight Z . Dashed regions represent filled states up to the chemical potential μ (dotted line).

We would like to stress that the phenomenological model described by Eqs. (4) and (5) is not meant at all to be exhaustive of the complex physics of a strongly correlated system. In fact, retardation effects are neglected, since we are assuming the separation into two species of electrons to be independent of frequency. More sophisticated methods of solution, including DMFT, permit one to treat the self-energy of a strongly correlated system in a more careful way, retaining the correct frequency dependence of the self-energy.

Our model has the advantage of being extremely simple and easy to handle, and it allowed us to obtain explicit expressions for all the relevant quantities of the coupled electron-phonon system; in particular, we focus on the spectral weight transfer from the coherent to the incoherent part of the Green's function when increasing the degree of electronic correlation. As we are going to see, this feature will have important consequences on the electronic screening and on the momentum dependence of the electron-phonon coupling.

III. SCREENING AND ELECTRON-PHONON INTERACTION

A. Correlation effects on Thomas-Fermi screening

The momentum dependence of the electron-phonon interaction usually plays a marginal role in determining the electron-phonon properties of common metals. The basic reason for this is that the bare long-range electron-phonon interaction is effectively screened by the long-range Coulomb repulsion leading to a weak momentum dependence.

The conventional Migdal-Eliashberg theory, which describes electron-phonon effects of both the normal and the superconducting states, is formally derived starting from an effective electron-phonon Hamiltonian, in which the Coulomb electron-electron repulsion does not appear, apart from a weak residual electron-electron contribution in the Cooper channel, $U_{\mathbf{k}, \mathbf{q}}$, which gives rise to the Morel-Anderson "pseudopotential" term $\mu = N(0)U$.³² The physical quantities appearing in this effective Hamiltonian are thus considered to have been already renormalized by the long-range Coulomb interaction. In particular the electron-phonon matrix elements $g_{\mathbf{k}, \mathbf{k}+\mathbf{q}}$ and the residual electron-electron repul-

sion are usually considered to have a negligible momentum dependence, so that the Eliashberg equations depend only on the frequency variables.

This drastic assumption works quite well in many conventional low-temperature superconductors with large carrier density since, in this case, the long-range \mathbf{q} dependence of the bare electron-phonon and electron-electron interaction [$V(\mathbf{q}, \omega) \propto 1/|\mathbf{q}|^2$] is removed by the large metallic screening. This well-known effect is usually expressed in terms of the (static) dielectric function $\epsilon(\mathbf{q})$, which in the random-phase approximation (RPA) reads

$$\epsilon(\mathbf{q}) = 1 + \frac{k_{\text{TF}}^2}{|\mathbf{q}|^2}, \quad (6)$$

where k_{TF} is the Thomas-Fermi screening momentum defined as

$$k_{\text{TF}}^2 = -\lim_{\mathbf{q} \rightarrow 0} 4\pi e^2 \Pi(\mathbf{q}, \omega=0), \quad (7)$$

with

$$\Pi(\mathbf{q}, \omega) = \frac{2}{N_s} \sum_{\mathbf{k}} \int d\omega' G(\mathbf{k} + \mathbf{q}, \omega + \omega') G(\mathbf{k}, \omega'). \quad (8)$$

The effective long-range interaction results thus screened by conduction charge and one obtains the following Thomas-Fermi expression:

$$V_{\text{eff}}(\mathbf{q}, \omega) = \frac{V(\mathbf{q}, \omega)}{\epsilon(\mathbf{q})} \propto \frac{1}{|\mathbf{q}|^2 + k_{\text{TF}}^2}. \quad (9)$$

In free-electron systems the Thomas-Fermi vector is directly related to the bare density of states via the simple relation $\lim_{\mathbf{q} \rightarrow 0} \Pi(\mathbf{q}, \omega=0) = -2N(0)$, where $N(0)$ is the density of states per spin at the Fermi level, so that $k_{\text{TF}}^2 = 8\pi e^2 N(0)$. In common metals, since k_{TF} is typically larger than the Brillouin-zone size (k_{BZ}), the effective (electron-electron, electron-phonon) interaction $V_{\text{eff}}(\mathbf{q}, \omega)$ can be considered in first approximation to the almost independent of the exchanged momentum \mathbf{q} .

Things are expected to be very different in correlated, narrow-band systems. As we have mentioned before, strongly correlated electrons, due to their reduced mobility, are much less effective in screening external perturbations, especially at small wavelengths. For instance, the reduction of the screening properties approaching a metal-insulator transition in disorder alloys as well as in cuprates has been experimentally signaled in Refs. 40,41.

In this section we employ the simple model introduced above for the description of the Green's function to quantify the reduced screening properties of correlated systems and their dependence on microscopic parameters, such as the hole doping δ or the Hubbard repulsion U . In order to do this, we compute the Thomas-Fermi vector k_{TF} , defined in Eq. (7), using the model described by Eqs. (4) and (5) to evaluate the RPA response function $\Pi(\mathbf{q}, \omega)$ according to Eq. (8). While higher-order (vertex) diagrams are not taken into account in this framework, we shall show that this simple

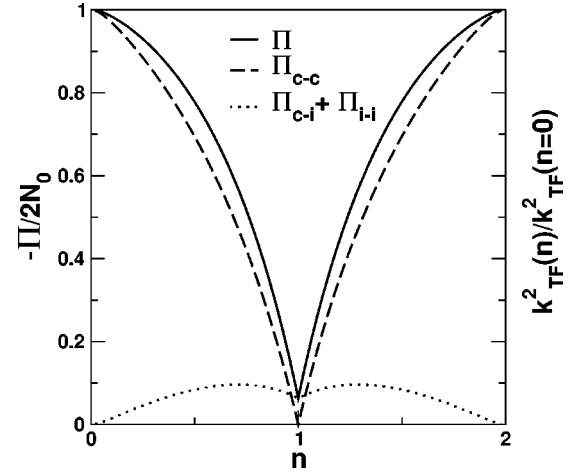


FIG. 3. Effective Thomas-Fermi screening k_{TF}^2 (solid line) as a function of the electron density n for a correlated system described by our model ($U=8U_c$). The different contributions to the total screening are also shown: coherent-coherent particle-hole processes (dashed line) and coherent-incoherent + incoherent-incoherent contribution (dotted line). Apart from half filling, where the coherent contribution vanishes and the screening is determined by the only residual incoherent polarization, the static screening properties of the system are dominated from the coherent quasiparticle excitations.

model is already sufficient to describe the reduction of screening properties due to transfer of spectral weight from the coherent to the incoherent states.

Using Eqs. (4) and (5) the response function Π can be written as a sum of three different contributions:

$$\Pi = \Pi_{c-c} + \Pi_{c-i} + \Pi_{i-i}, \quad (10)$$

where the first one describes scattering processes which involve only coherent states; the second term describes scattering between the coherent peak and the Hubbard lower/upper (incoherent) bands; the last one describes processes which involve only localized incoherent states in both the Green's functions of Eq. (8). In general we expect that the total screening will be dominated by the first contribution Π_{c-c} since the itinerant coherent states are much more effective, because of their mobility, in screening external perturbations than the localized ones.

In Fig. 3 we plot the RPA response function in units of the bare DOS: $-\lim_{\mathbf{q} \rightarrow 0} \Pi(\mathbf{q}, \omega=0)/2N_0$ as a function of the electron filling. Since for $n \rightarrow 0$ the screening properties are determined only by the coherent part regardless of any correlation effects, this is also equivalent to plotting the Thomas-Fermi momentum k_{TF}^2 as function of the electron density n : $k_{\text{TF}}^2(n)/k_{\text{TF}}^2(n=0)$. As shown in Fig. 3 the net value of the Thomas-Fermi momentum is mainly determined by the coherent-coherent excitations. Simple scaling considerations show that the coherent-coherent contribution to the response function is just equal to \sqrt{Z} times the Thomas-Fermi momentum of an uncorrelated system. The explicit expressions of the other two terms are a bit more complicated and they are reported in Appendix B. Figure 3 shows a drastic reduction of the screening properties of the system as

the metal-insulator transition is approached at half filling ($U > U_c$). In this case the spectral weight of the coherent part is zero, and the only residual small contribution to the screening is due to incoherent excitations which vanish for $U \rightarrow \infty$.

B. Poor screening and momentum dependence of the electron-phonon interaction

From Fig. 3 it is clear that the assumption of a Thomas-Fermi momentum much larger than the exchanged phonon momenta \mathbf{q} breaks down as electronic correlation effects get more and more relevant, namely, approaching half filling. In this situation the effective electron-phonon interaction can be no longer considered weakly dependent on \mathbf{q} in the long-range limit $\mathbf{q} \rightarrow 0$. On a microscopical ground the screening of long-range Coulomb interaction renormalizes both the bare electron-phonon matrix element $g_{\mathbf{k}, \mathbf{k}+\mathbf{q}}^0$ and the phonon frequencies $\Omega_{\mathbf{q}}$. The el-ph matrix element can be usefully written as $g_{\mathbf{k}, \mathbf{k}+\mathbf{q}}^0 \approx c(\Omega_{\mathbf{q}})/|\mathbf{q}|$, where $c(\Omega_{\mathbf{q}})$ is a well behaved function of \mathbf{q} in the limit $\lim_{\mathbf{q} \rightarrow 0}$ and it mainly depends on the phonon frequency $\Omega_{\mathbf{q}}$. If both the screening effects on $g_{\mathbf{k}, \mathbf{k}+\mathbf{q}}^0$ and $\Omega_{\mathbf{q}}$ are properly taken into account³³ one can get the following expression for the effective total electron-phonon interaction:

$$V_{\text{eff}}^{\text{el-ph}}(\mathbf{q}, \omega) = \frac{c^2(\omega_{\mathbf{q}})}{|\mathbf{q}|^2 \epsilon(\mathbf{q})} D_{\mathbf{q}}(\omega), \quad (11)$$

where both the phonon propagator $D_{\mathbf{q}}(\omega)$ and the coupling function $c(\omega_{\mathbf{q}})$ are written in terms of the screened phonon frequency $\omega_{\mathbf{q}}$. Equation (11) shows that the long-range behavior of the total el-ph interaction $\propto 1/|\mathbf{q}|^2$, when written as function of the screened phonon frequency, is correct by the dielectric function $\epsilon(\mathbf{q})$.

For an optical mode, $\omega_{\mathbf{q}}$ is only weakly dependent on \mathbf{q} and the leading dependence on \mathbf{q} of Eq. (11) comes from the term $\propto 1/[\epsilon(\mathbf{q})|\mathbf{q}|^2]$. These screening effects can be conveniently dealt with by introducing the screened el-ph matrix element $g_{\mathbf{q}}$:

$$g_{\mathbf{q}}^2 = \frac{|g_{\mathbf{q}}^0|^2}{\epsilon(\mathbf{q})} \propto \frac{1}{|\mathbf{q}|^2 + k_{\text{TF}}^2}. \quad (12)$$

The el-ph scattering is thus roughly described (we remind that these expression were derived in the limit $\mathbf{q} \rightarrow 0$) by a Lorentzian function in the space $|\mathbf{q}|$. It is also useful to introduce the dimensionless variables $Q = |\mathbf{q}|/2k_{\text{F}}$ and $Q_c = k_{\text{TF}}/2k_{\text{F}}$, so that

$$|g(Q)|^2 \approx g^2 \frac{1}{Q^2 + Q_c^2}. \quad (13)$$

The parameter Q_c represents a cutoff for the exchanged phonon momenta: the electron-phonon scattering will be operative for $Q \lesssim Q_c$, and negligible for $Q \gtrsim Q_c$.

The momentum structure resulting in Eq. (13) plays a crucial role in the Cooper pairing in the coherent-coherent channel where the momentum is a good quantum number.

For these contributions the total strength of the electron-phonon coupling is linked with the momentum average of Eq. (11) over the Fermi surface. For an isotropic system, using polar coordinates $\int d\Omega = \int_0^{2\pi} d\phi \int_0^1 d \cos \theta$ and reminding that $Q = \sin(\theta/2)$, we obtain

$$\langle |g(Q)|^2 \rangle_{\text{FS}} = \frac{\int d\phi \int_0^1 Q dQ \frac{g^2}{Q^2 + Q_c^2}}{\int d\phi \int_0^1 Q dQ} = g^2 \ln \left(\frac{1 + Q_c^2}{Q_c^2} \right). \quad (14)$$

In common metals $Q_c \sim 0.5-1$ so that $\ln[(1+Q_c^2)/Q_c^2]$ is of the order of 1. On the other hand, in poorly screened systems $Q_c \ll 1$ and the resulting el-ph coupling is sensibly enhanced. In the following, we shall consider $Q_c \approx 0.7$ as a representative case of uncorrelated usual metals.

For practical purposes, following Refs. 18,19, we approximate the Lorentzian behavior of Eq. (13) with a Heaviside θ function:

$$|g(Q)|^2 \rightarrow g^2 \alpha \theta(Q_c - Q). \quad (15)$$

In order to preserve in this mapping the total strength of the el-ph coupling, the prefactor α has to be determined by requiring the resulting el-ph coupling strength, namely, the average of g^2 over the Fermi surface, to be equal for Eqs. (13) and (15). With this condition we find that

$$|g(Q)|^2 = g^2 \frac{1}{Q_c^2} \ln \left(\frac{1 + Q_c^2}{Q_c^2} \right) \theta(Q_c - Q). \quad (16)$$

As a final remark of this section we note that the momentum dependence of $|g(Q)|^2$ is not expected on the other hand to be effective in the incoherent-coherent and incoherent-incoherent contributions to the electron-phonon interaction, where the exchanged momentum \mathbf{q} is no more a good quantum number. In this case the effective incoherent electron-phonon coupling is roughly given by its momentum average on the Brillouin zone, which we shall set in the following discussion to be equal to g^2 .

IV. GENERALIZED MIGDAL-ELIASHBERG EQUATIONS

In the previous sections we have introduced a simple model for an electron-phonon system in the presence of electronic correlation. In particular we have reduced, in an approximate way, the complex problem of the interplay between electron-phonon and electron-electron interactions to a purely electron-phonon system described by an effective one-particle Green's function [Eqs. (1), (4), and (5)] and an effective electron-phonon matrix element $g(Q)$ [Eq. (16)]. After this mapping, the Baym-Kadanoff theory³⁵ assures that the functional form of the superconducting equations will be the same as that of a purely electron-phonon system:

$$\Phi = \Phi_{\text{el-ph}}[g, G, \Phi], \quad (17)$$

$$Z = Z_{\text{el-ph}}[g, G, \Phi], \quad (18)$$

where Φ is the superconducting order parameter; the Green's function G and the matrix element g are defined by Eqs. (1), (4), (5), and (16), as mentioned above. In order to obtain an explicit expression for Eqs. (17) and (18) we should specify *in which framework* we are going to treat the electron-phonon interaction. In particular, we observe that the conventional ME theory, in particular, is based on the assumption that the phonon frequencies are much smaller than the electronic Fermi energy, $\omega_{\text{ph}} \ll E_F$ (adiabatic limit). This theory works quite well in the conventional low-temperature superconductors, where no electronic correlation is present and E_F is of the order of 5–10 eV. On the other hand, the strong band renormalization in correlated systems described in Sec. II questions the adiabatic assumption, especially as, approaching half filling, the renormalized bandwidth $\sim ZE$ can be comparable with ω_{ph} . In these systems a more suitable description can be obtained in the framework of the nonadiabatic theory of superconductivity.^{17–19} Equations (17) and (18) can be rewritten as

$$Z_n = 1 + \frac{T_c}{\omega_n} \sum_m \Gamma_Z([G]; \omega_n, \omega_m) \eta_m[G], \quad (19)$$

$$\Phi_n = T_c \sum_m \Gamma_\Phi([G]; \omega_n, \omega_m) \frac{\Phi_m}{\omega_m Z_m} \eta_m^\Delta[G], \quad (20)$$

where the electron-phonon kernels $\Gamma_Z([G]; \omega_n, \omega_m)$ and $\Gamma_\Phi([G]; \omega_n, \omega_m)$ contain the nonadiabatic vertex (P) and cross (C) contributions to the self-energy and to the Cooper pairing channels:

$$\Gamma_Z([G]; \omega_n, \omega_m) = \lambda_{n-m} [1 + \lambda P([G]; \omega_n, \omega_m, Q_c)],$$

$$\Gamma_\Phi([G]; \omega_n, \omega_m) = \lambda_{n-m} [1 + 2\lambda P([G]; \omega_n, \omega_m, Q_c)] \\ + \lambda^2 C([G]; \omega_n, \omega_m, Q_c) - \mu.$$

Here λ_{n-m} is linked with the electron-phonon spectral function $\alpha^2 F(\omega)$ through the relation $\lambda_{n-m} = 2 \int d\omega \alpha^2 F(\omega) \omega / [\omega^2 + (\omega_n - \omega_m)^2]$, $\lambda = \lambda_{n-m=0}$, and μ is the short-range residual electron-electron repulsion. The breakdown of the adiabatic hypothesis determines the need for the explicit inclusion of the vertex (P) and cross (C) functions in Eqs. (19) and (20) and it affects the expression of $\eta_m[G] = \sum_{\mathbf{k}} G(\mathbf{k}, \omega)$ and $\eta_m^\Delta[G] = \sum_{\mathbf{k}} G(\mathbf{k}, \omega) G(-\mathbf{k}, -\omega)$ through finite bandwidth effects. The momentum dependence of the superconducting equations has been averaged on the Fermi surface and it gives rise to the strong dependence on Q_c in the vertex and cross terms. In Eqs. (19) and (20) we have moreover implicitly expressed the functional dependence of the electron-phonon kernels Γ_Z and Γ_Δ as well as of the quantities P , C , and η on the Green's function G which, we remind, is modeled as in Eqs. (1), (4), and (5).

Before solving Eqs. (19) and (20) in the whole range of doping, we would like to discuss the different roles of the coherent (itinerant) states and the incoherent (localized) states, described, respectively, by Eqs. (4) and (5), on the superconducting properties. As we have seen in Sec. III, the electronic screening is mainly dominated by the coherent

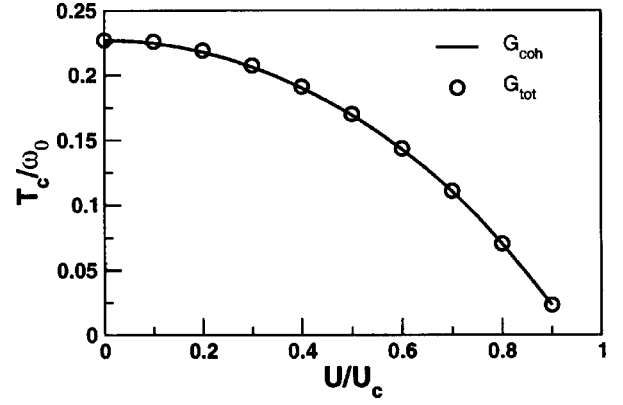


FIG. 4. Comparison of the critical temperature T_c as a function of U for the half filling case, using the full integral kernel in Eqs. (19)–(20) (empty circles) and using only its coherent part (solid line).

term of the electronic Green's function, which describes mobile electrons for which \mathbf{k} is a good quantum number.

Similar considerations can be made also for superconductivity: we expect, in fact, that the coherent electrons, which have a high mobility, will give a more relevant contribution to the superconducting critical temperature. To check the validity of this hypothesis, we have solved Eqs. (19) and (20) in the ME limit (i.e., neglecting vertex corrections), once using an integral kernel containing the full Green's function [Eq. (1)] and once an integral kernel with only the coherent part of the Green's function [Eq. (4)], as a function of the Hubbard repulsion U . In Fig. 4, we show as empty circles the results obtained with the full kernel, and with solid line the critical temperature obtained using only the coherent part. The two sets of data are hardly distinguishable, pointing out that the increase of T_c due to the coherent-incoherent and incoherent-incoherent couplings is negligible.

After this observation, in the following, the functional dependence on the total Green's function G in Eqs. (19) and (20) can be in good approximation replaced by the only coherent part, explicitly: $\Gamma_Z[G_{\text{coh}}]$, $\Gamma_\Phi[G_{\text{coh}}]$, $P[G_{\text{coh}}]$, $C[G_{\text{coh}}]$, $\eta_m[G_{\text{coh}}]$. As we show in Appendix B, when the reduced spectral weight and bandwidth are taken into account, this corresponds to a proper rescaling of the analytical expressions for these quantities evaluated in the absence of correlation in Refs. 36,37.

It is interesting to compare our model with the two-band superconductivity,³⁸ which has recently driven a considerable attention due to MgB_2 .³⁹ In that case, the opening of interband scattering channels leads to an enhancement of the critical temperature. In some respects, our model could also be seen as an effective two-band system, made up of a very narrow band of mobile electrons and another band of localized electrons, coupled to each other. However, we note that, since the spectral weight of each single band is not conserved, the onset of the high-energy bands of localized electrons is accompanied by a decrease of the quasiparticle spectral weight, resulting in an effective reduction of the Cooper pairing.

A. Doping effects and phase diagram of the nonadiabatic superconductivity

Equations (19) and (20) represent our tool to investigate the loss of the superconducting properties due to the electronic correlation approaching half filling. We can in fact evaluate all the relevant quantities, such as the electron-phonon interaction kernels Γ_Z , Γ_Δ , the electron Green's function G , the vertex and cross functions P , C , and the momentum cutoff Q_c as a function of the microscopic parameters as the hole doping δ and the Hubbard repulsion U . We shall show that the phase diagram as a function of the doping is governed by two competing effects: one driven by the reduction of the coherent spectral weight approaching half filling, which is detrimental for superconductivity, and the other by the complex behavior of the nonadiabatic terms, which increases the effective pairing as $\delta \rightarrow 0$ and decreases it as $\delta \rightarrow 1$.

Since we are mainly interested in the region $\delta \rightarrow 0$ of the phase diagram, we disregard for simplicity the analytical dependence of the nonadiabatic terms on the chemical potential. The behavior of the "bare" P and C as a function of doping is in fact determined by the density of electrons ($n = 1 - \delta$); this dependence is much weaker than the dependence of Z and Q_c close to half filling (see Figs. 3 and 1).

Before solving Eqs. (19) and (20) numerically to obtain the critical temperature T_c as a function of doping, we wish to discuss the phase diagram of our model in terms of simple intuitive physical arguments, based on an effective electron-phonon coupling. Let us consider for the moment the electron-phonon interaction alone, without any residual Coulomb repulsion, namely, $\mu = 0$. Equation (20) can be rewritten in a simplified way as

$$\Phi_n \simeq T_c \sum_m Z\lambda [1 + 2Z\lambda P + Z\lambda C] K_{n-m} \Phi_m, \quad (21)$$

where we have simplified, according to Appendix B, the main dependences on $Z = Z(U, \delta)$ of each quantity. In this way, we can roughly see the total electron-phonon coupling as the product of two terms: an effective electron-phonon coupling of ME theory renormalized by the electronic correlation, λ^{ME} , and the enhancement due to nonadiabatic vertex and cross (VC) diagrams γ^{VC} :

$$\lambda^{\text{eff}} = \lambda^{\text{ME}} \gamma^{\text{VC}},$$

$$\lambda^{\text{ME}} = Z\lambda,$$

$$\gamma^{\text{VC}} = 1 + 2Z\lambda P(Q_c) + Z\lambda C(Q_c).$$

The schematic behavior of these quantities as a function of the hole doping δ is shown in the upper panel of Fig. 5. The physics behind the δ dependence of λ^{ME} can be easily related to the loss of spectral weight approaching the metal-insulator transition for $\delta \rightarrow 0$. This effect, which is present also in γ^{VC} , is however in that case competing with the enhancement of the effective coupling due to $P(Q_c)$ and $C(Q_c)$ which will be maximum and positive close to half filling (where $Q_c \rightarrow 0$) and negative at high dopings. The

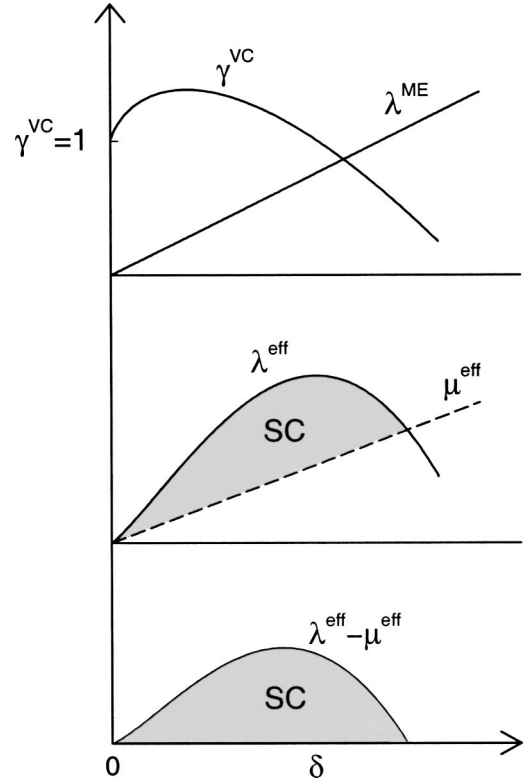


FIG. 5. Graphical sketch of the different contributions to the effective superconducting coupling. Top panel: the coupling function λ^{ME} is mainly determined by the coherent spectral weight, and it exhibits a monotonous growing behavior as a function of doping. The vertex factor γ^{VC} tends to enhance the effective coupling at low doping and to depress it at high doping. Middle panel: the total effective electron-phonon coupling $\lambda^{\text{eff}} = \lambda^{\text{ME}} \gamma^{\text{VC}}$ has a maximum at some finite value of δ ; when the effective Morel-Anderson pseudopotential is subtracted, superconductivity is suppressed at high doping. Lower panel: resulting phase diagram for superconductivity: superconductivity is only possible in a finite region of phase space (gray region), where $\lambda^{\text{eff}} - \mu^{\text{eff}}$ is positive.

interplay between these two effects will give rise to a maximum of γ^{VC} , and hence of λ^{eff} , somewhere in the small doping region where the competition between the spectral weight loss and the positive nonadiabatic effects is stronger (see upper and middle panels in Fig. 5).

We can now also consider the effect of the residual Morel-Anderson-like repulsion μ ; first of all, we observe that the reduction of spectral weight will lead to an effective repulsion $\mu^{\text{eff}} \simeq Z\mu$. Superconductivity will be possible only when the net electron-phonon attraction overcomes the repulsion term: $\lambda^{\text{eff}} - \mu^{\text{eff}} > 0$ (see lower panel of Fig. 5). The resulting total coupling is expected to exhibit a "bell" shape which is mostly due to the δ dependence of the nonadiabatic factor γ^{VC} . It is interesting to note two things. First, in the extreme case $\lambda^{\text{ME}} \leq \mu^{\text{eff}}$, where no superconductivity would be predicted in the whole δ range by the conventional ME theory, we could expect finite T_c in a small δ region, due to purely nonadiabatic effects $\lambda^{\text{eff}} = \lambda^{\text{ME}} \gamma^{\text{VC}} > \mu^{\text{eff}}$. Second, it is clear that within the ME framework a net attractive interaction in the Cooper channel at a certain doping δ , which corresponds

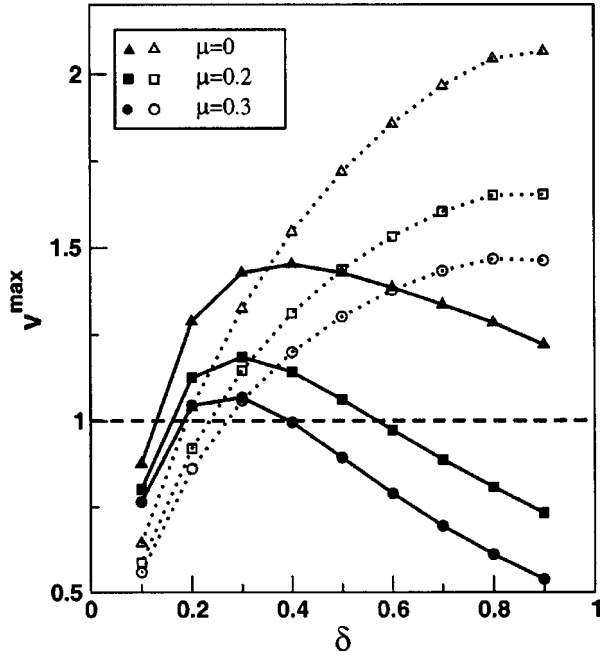


FIG. 6. Maximum eigenvalue v^{\max} as a function of doping, evaluated at $T=0.01\omega_0$ for different values of μ , with $\lambda=1$, $\omega_0=0.8E/2$, and $U=8U_c$. Empty symbols (dashed lines) represent ME theory, filled symbols (solid lines) the nonadiabatic theory described by Eqs. (19)–(20).

to $\lambda^{\text{ME}} > \mu^{\text{eff}}$, would imply a superconducting order also at larger δ since the two quantities $\lambda^{\text{ME}}, \mu^{\text{eff}}$ scale in the same way $\propto Z$; on the other hand, in the nonadiabatic theory superconductivity, T_c is expected to be limited to some maximum value of doping, due to the negative contribution of the nonadiabatic diagrams P and C at large δ (large Q_c 's).

We can now quantify the simple arguments discussed so far. A quantitative estimate of the strength of the superconducting pairing is given by the highest eigenvalue v^{\max} of the superconducting integral kernel in Eq. (20), computed at low T ; at a given temperature T and doping δ superconductivity occurs if $v^{\max} \geq 1$ and the superconducting pairing (and T_c) is stronger as v^{\max} is larger.

In Fig. 6 we compare the behavior of v^{\max} as a function of δ , obtained at $T=0.01\omega_0$ using an Einstein spectrum for different values of μ in ME (open symbols, dashed lines) and in the nonadiabatic theory (full symbols, solid lines). The Hubbard repulsion was set at $U=8U_c$ and the phonon frequency at $\omega_0=0.8E/2$, where $E/2$ is the bare half-bandwidth (unrenormalized by correlation effects). The corresponding phase diagram T_c versus δ is reported in Fig. 7. In agreement with our previous discussion in the ME framework v^{\max} and T_c decrease monotonously as the hole doping is reduced. On the other hand, the corresponding results in the nonadiabatic theory display a more complex behavior, showing that the effective nonadiabatic pairing is larger than the ME one at low doping and smaller at high doping.

As we have already discussed, the bell shape of the high-est eigenvalue v^{\max} and of the critical temperature T_c can be attributed to the dependence of the magnitude and sign of the nonadiabatic terms on Q_c , which, in turn, strongly depends

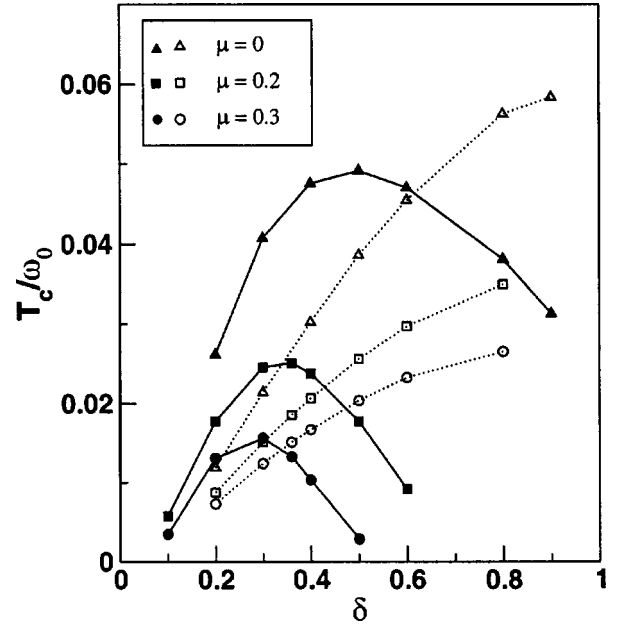


FIG. 7. Phase diagram of T_c vs δ for the adiabatic (empty symbols, dashed lines) and nonadiabatic (filled symbols, solid lines) theory. Details as in Fig. 6.

on doping. For high doping the nonadiabatic contributions are negative and decrease v^{\max} and T_c with respect to their ME values. On decreasing δ the nonadiabatic terms turn from negative into positive and v^{\max} and T_c increase up to a maximum value. As the hole doping is further decreased ($\delta \rightarrow 0$), the loss of spectral weight becomes the dominant effect and it finally leads to the complete suppression of superconductivity. The inclusion of the residual Coulomb repulsion in the Cooper channel, μ , leads to an overall reduction of the superconducting pairing. The effect is more pronounced in the nonadiabatic theory than in ME, since in this case a very small value of μ is enough to suppress superconductivity in a large region of phase space at high dopings.

V. DISCUSSION AND CONCLUSIONS

The main aim of the present paper is the description, on microscopical grounds, of the hole doping dependence of the electron-phonon and superconducting properties of a strongly correlated system within the context of a nonadiabatic electron-phonon theory. The need for a nonadiabatic treatment of the electron-phonon interaction in correlated systems comes from the fact that, as a metal-insulator transition is approached, the electronic bandwidth is strongly reduced, and the adiabatic assumption ω_{ph}/E_F on which Migdal's theorem is based breaks down.

Past studies have shown that the inclusion of nonadiabatic effects can lead to a strong enhancement or depression of T_c depending on the value of the exchanged momenta and frequencies: if a microscopic mechanism leads to a predominance of the forward scattering in the electron-phonon interaction, T_c is strongly enhanced. This effect was schematized in the past with the introduction of an effective cutoff in the electron-phonon interaction (Q_c), which was argued to be

due to strong correlations effects.

In this work we have related the existence of Q_c with the reduction of the screening properties due to correlation of a metal approaching a metal-insulator transition. The same effects which are responsible for the reduction of the screening (namely, the loss of \mathbf{k} -space coherence) are however also strongly detrimental to superconductivity. In this work we have analyzed how the interplay between these effects is reflected on a T_c versus doping phase diagram.

We have introduced a simple analytical model to simulate the effects of the strong correlation on the one-electron Green's function. This model has also been employed to estimate the role of the electronic screening on the electron-phonon scattering in correlated systems. We have shown that the reduction of the metallic character due to the electronic correlation implies a reduction of the "effective" Thomas-Fermi screening approaching $\delta=0$, where correlation is stronger. This results in a predominance of forward (small- \mathbf{q}) scattering, which has been parametrized in terms of a phonon momentum cutoff $Q_c = k_{TF}/2k_F$, where k_{TF} and k_F are, respectively, the Thomas-Fermi and the Fermi vectors.

We have also shown how the different parts of the electronic Green's function contribute to the superconducting pairing; in particular, we have shown that the superconducting critical temperature is mainly determined by the coherent excitations. The similarities and differences between our model and the two-band superconductivity^{38,39} have also been discussed.

Solving the nonadiabatic generalized ME equations, we obtained a T_c versus δ diagram, which can be ideally divided into three regions.

(a) A high doping region, where superconductivity is suppressed by the negative contribution of the nonadiabatic channels to the electron-phonon pairing.

(b) An extremely low doping region, where the poor metallic character is reflected in a vanishing coherent spectral weight. In this region, superconductivity is extremely unstable and it can be overwhelmed by other electronic or structural instabilities induced by spin and charge degrees of freedom (antiferromagnetic fluctuations, stripes, charge-density waves, pseudogaps, . . .).

(c) An intermediate doping region, in which the loss of coherent spectral weight is not large enough to prevent superconductivity, which is in turn enhanced by the positive contribution of the nonadiabatic channels of interactions.

The resulting phase diagram bears strong resemblance with that of cuprates. We have in fact an overdoped region, where superconductivity is triggered on by the positive contribution of the nonadiabatic channels as doping is decreased; an optimal doping region, where the enhancement due to the nonadiabatic interaction is counterbalanced by the reduction of the metallic character; and an underdoped region, where superconductivity disappears due to the incipient metal-insulator transition. In the qualitative scenario outlined here the origin of superconductivity in cuprates can be understood by focusing on the overdoped region, where the materials retain defined metallic properties; on the other hand, the exotic phenomenology of the underdoped region is only marginal. The occurrence of different kinds of

electronic/structural instabilities, not discussed in the present paper, is thus thought to be a byproduct of the loss of metallic character, which also drives the *suppression* of T_c as $\delta \rightarrow 0$, more than the secret of the superconducting pairing.

Once more, we wish to stress that what we present in this paper is a general scenario, based on the microscopical description of the interplay between nonadiabatic effects and strong electronic correlation. A quantitative understanding of the specific phase diagram of cuprates should of course take into account specific features of these materials, such as Van Hove singularities and the d -wave symmetry of the gap. The possibility of a d -wave pairing within the context of electron-phonon superconductivity has been discussed elsewhere;²⁵ we remind here that d -wave symmetry was shown to be favored by forward scattering, which in our model is enhanced as $\delta \rightarrow 0$.

The qualitative behavior of our results would be however left unchanged by the inclusion of these effects.

On the experimental ground we observe that the present scenario is supported by a detailed analysis of T_c versus normal-state properties in different families of cuprates. In Ref. 40, for example, the complex behavior of T_c approaching the metal-insulator transition either by reducing the doping or by increasing the disorder was nicely pointed out by Osofsky *et al.* The relation between T_c and reduced screening properties was also discussed there. Although we do not attempt to discuss the scaling relations close to the metal-insulator transition in region (b), where a more specific treatment of the electronic correlation is needed, we think our analysis is somehow complementary to that of Ref. 40. This scenario can also open new perspectives on the remarkable increase of T_c in granular metals and alloys.⁴¹

Furthermore, a strong doping dependence of the electron-phonon properties in cuprates has also been reported by inelastic x-ray measurements of the phonon dispersion.⁶ Experimental data in Nd-based compounds were shown to be compatible with the theoretical calculations, based on the shell model, assuming a negligible Thomas-Fermi vector ($Q_c=0$) for the strongest correlated undoped compound ($\delta=0$), whereas a Thomas-Fermi momentum $k_{TF} \approx 0.39 \text{ \AA}^{-1}$, comparable to that for La-based compounds, was estimated for $\delta \approx 0.14$. The corresponding dimensionless cutoff Q_c would be hence estimated, $Q_c \approx 0.26$, by using an in-plane Fermi vector $k_F^{ab} \approx 0.74 \text{ \AA}^{-1}$.³⁴

ACKNOWLEDGMENTS

L.B. wishes to thank Massimo Capone and Giorgio Sant'Agostino for useful discussion and comments. The authors acknowledge financial support by the MIUR projects COFIN2001 and FIRB-RBAU017S8R, and by the INFN project PRA-UMBRA.

APPENDIX A: GUTZWILLER SOLUTION FOR GENERIC U AND n

In this appendix we provide a brief overview of the analytical solution of the Gutzwiller approximation for generic filling and Hubbard repulsion.

Let us write the Hubbard Hamiltonian within the Gutzwiller approximation (in the paramagnetic state) as

$$H = -\gamma(U, n, d)|\bar{\epsilon}| + Ud, \quad (\text{A1})$$

where n is the total electron filling, d the density of double occupancy sites, $\bar{\epsilon}$ the kinetic energy for site, and

$$\gamma(U, n, d) = \frac{2(n-2d)}{n(2-n)} [\sqrt{1-n+d} + \sqrt{d}]^2. \quad (\text{A2})$$

Minimizing Eq. (A1) with respect to d yields

$$0 = [\sqrt{1-n+d} + \sqrt{d}]^2 - \left(\frac{n}{2} - d\right) \frac{[\sqrt{1-n+d} + \sqrt{d}]^2}{\sqrt{d(1-n+d)}} + 2\left(\frac{U}{U_c}\right)n(2-n), \quad (\text{A3})$$

where we have introduced as usual $U_c = 8|\bar{\epsilon}|$.

After expanding the squares $[\sqrt{\dots} + \sqrt{\dots}]^2$ one can now isolate on the right-hand side the remaining square roots:

$$2n(2-n)\left(\frac{U}{U_c}\right) + (1-2n+4d) = \left(\frac{n}{2} - d\right) \frac{(1-n+2d)}{\sqrt{d(1-n+d)}} - 2\sqrt{d(1-n+d)}, \quad (\text{A4})$$

and, by squaring both the sides of Eq. (A4), all the remaining square roots are removed and we are left with a third-order polynomial expression for d . We obtain

$$A_3 d^3 + A_2 d^2 + A_1 d + A_0 = 0, \quad (\text{A5})$$

where

$$A_3 = 16n(2-n)\left(\frac{U}{U_c}\right), \quad (\text{A6})$$

$$A_2 = 4n(2-n)\left(\frac{U}{U_c}\right) \left[n(2-n)\left(\frac{U}{U_c}\right) - 6n + 5 \right], \quad (\text{A7})$$

$$A_1 = (1-n) \left[4n^2(2-n)^2 \left(\frac{U}{U_c}\right)^2 + 4n(2-n)(1-2n)\left(\frac{U}{U_c}\right) - n \right], \quad (\text{A8})$$

$$A_0 = -\frac{n^2(1-n)^2}{4}. \quad (\text{A9})$$

Equation (A5) can be easily solved to obtain d_{\min} , and, in the standard notations, the Gutzwiller factor $Z(U, n) = \gamma(U, n, d_{\min})$.

APPENDIX B: ANALYTICAL EXPRESSION OF DIFFERENT PHYSICAL QUANTITIES

1. Thomas-Fermi Screening

In this section we provide some useful analytical expressions for the different contributions (Π_{c-c} , Π_{c-i} , Π_{i-i}) to the response function Π involved in the evaluation of the Thomas-Fermi screening as limit $k_{\text{TF}}^2 \propto \lim_{\mathbf{q} \rightarrow 0} \Pi(\mathbf{q}, \omega = 0)$.

In the RPA approximation $\Pi(\mathbf{q}, \omega)$ is given by

$$\Pi(\mathbf{q}, \omega) = \frac{2}{N_s} \sum_{\mathbf{k}} \int d\omega' G(\mathbf{k} + \mathbf{q}, \omega + \omega') G(\mathbf{k}, \omega'). \quad (\text{B1})$$

We employ the simple model of Eqs. (1), (4), and (5) for the electron Green's function in the presence of correlation.

From simple scaling relation it is straightforward to recognize that

$$\Pi_{c-c} = Z\Pi(Z=0) = -ZN_0. \quad (\text{B2})$$

The analytical expressions for Π_{c-i} , Π_{i-i} are straightforward but more cumbersome since they involve the explicit integration over the upper/lower Hubbard bands. One obtains

$$\begin{aligned} \Pi_{c-i} = & -2N(0)^2(1-Z) \left\{ \left[ZE/2 + U/2 + \left(1 - \frac{n}{2}\right)E/2 \right] \ln \left[ZE/2 + U/2 + \left(1 - \frac{n}{2}\right)E/2 \right] \right. \\ & - \left[ZE/2 + U/2 - \left(1 - \frac{n}{2}\right)E/2 \right] \ln \left[ZE/2 + U/2 - \left(1 - \frac{n}{2}\right)E/2 \right] - \left[U/2 + \mu + \left(1 - \frac{n}{2}\right)E/2 \right] \ln \left[U/2 + \mu + \left(1 - \frac{n}{2}\right)E/2 \right] \\ & + \left[U/2 + \mu - \left(1 - \frac{n}{2}\right)E/2 \right] \ln \left[U/2 + \mu - \left(1 - \frac{n}{2}\right)E/2 \right] + (U/2 + nE/4 + ZE/2) \ln(U/2 + nE/4 + ZE/2) \\ & - (U/2 - nE/4 + ZE/2) \ln(U/2 - nE/4 + ZE/2) - (U/2 + nE/4 - \mu) \ln(U/2 - nE/4 - \mu) \\ & \left. + (U/2 - nE/4 + \mu) \ln(U/2 - nE/4 + \mu) \right\}. \quad (\text{B3}) \end{aligned}$$

The incoherent-incoherent contribution gives

$$\begin{aligned} \Pi_{i,i} = & -2N_0^2(1-Z)^2\{(U+E/2)\ln(U+E/2) \\ & + (U-E/2)\ln(U-E/2) - [U+(n-1)E/2] \\ & \times \ln[U+(n-1)E/2] - (U+[1-n]E/2) \\ & \times \ln[U+(1-n)E/2]\}. \end{aligned}$$

2. Superconducting properties

Here we report the explicit expressions for the coherent contribution to different quantities in Eqs. (19) and (20).

Let us consider, for instance, $\eta_m[G_{\text{coh}}]$. In this case $\eta_m[G_{\text{coh}}] = \eta_m^\Delta[G_{\text{coh}}]$ and

$$\begin{aligned} \eta_m[G_{\text{coh}}] &= \int d\epsilon N(\epsilon) \frac{Z}{i\omega_m - Z\epsilon_{\mathbf{k}} - \mu} \frac{Z}{-i\omega_m - Z\epsilon_{-\mathbf{k}} - \mu} \\ &= \frac{Z}{E\omega_m} \left[\arctan\left(\frac{ZE - \mu}{2\omega_m}\right) + \arctan\left(\frac{ZE + \mu}{2\omega_m}\right) \right]. \end{aligned} \quad (\text{B4})$$

Expression (B4) corresponds just to the $\eta_m(E)$ for an uncorrelated system with reduced spectral weight Z and rescaled bandwidth ZE : $\eta_m[G_{\text{coh}}](E) = Z\eta_m(ZE)$. Similar considerations apply for the vertex and cross function: $P[G_{\text{coh}}](E, Q_c; n, m) = ZP(ZE, Q_c; n, m)$, $C[G_{\text{coh}}](E, Q_c; n, m) = ZC(ZE, Q_c; n, m)$, where $P(E, Q_c; n, m)$ and $C(E, Q_c; n, m)$ in the absence of electronic correlation were computed in Refs. 17, 18, 36:

$$\begin{aligned} P(E, Q_c; n, m) &= T \sum_l D(\omega_n - \omega_l) \left\{ B(n, m, l) \right. \\ &+ \frac{A(n, m, l) - B(n, m, l)(\omega_l - \omega_{l-n+m})^2}{EQ_c^2} \\ &\times \left[\sqrt{1 + \left(\frac{2EQ_c^2}{\omega_l - \omega_{l-n+m}}\right)} - 1 \right. \\ &\left. \left. - \ln\left(\frac{1}{2} \sqrt{1 + \left(\frac{2EQ_c^2}{\omega_l - \omega_{l-n+m}}\right)^2}\right) \right] \right\}, \end{aligned} \quad (\text{B5})$$

$$\begin{aligned} C(E, Q_c; n, m) &= D(\omega_n - \omega_l) D(\omega_l - \omega_m) \\ &\times \left\{ 2B(n, -m, l) + \arctan\left(\frac{2EQ_c^2}{|\omega_l - \omega_{l-n+m}|}\right) \right. \\ &\left. \times \frac{A(n, -m, l) - B(n, -m, l)(\omega_l - \omega_{l-n-m})^2}{EQ_c^2 |\omega_l - \omega_{l-n-m}|} \right\}, \end{aligned} \quad (\text{B6})$$

where

$$\begin{aligned} A(n, m, l) &= (\omega_l - \omega_{l-n+m}) \left[\arctan\left(\frac{E}{2\omega_l}\right) \right. \\ &\left. - \arctan\left(\frac{E}{2\omega_{l-n+m}}\right) \right], \end{aligned} \quad (\text{B7})$$

$$\begin{aligned} B(n, m, l) &= (\omega_l - \omega_{l-n+m}) \frac{E\omega_{l-n+m}}{2[(E/2)^2 + \omega_{l-n+m}^2]^2} \\ &- \frac{E}{2[(E/2)^2 + \omega_{l-n+m}^2]}. \end{aligned} \quad (\text{B8})$$

¹M.K. Crawford, W.E. Farneth, E.M. McCarron, R.L. Harlow, and E.H. Moudden, *Science* **250**, 1390 (1990).

²J.P. Franck, S. Gyax, S. Soerensen, E. Altshuler, A. Hnatiw, J. Jang, M.A.-K. Mohamed, M.K. Yu, G.I. Sproule, J. Chrzanowski, and J.C. Irwin, *Physica C* **185–189**, 1379 (1991).

³See H. Keller, *Physica B* **326**, 283 (2003), and references therein.

⁴F. Raffa, T. Ohno, M. Mali, J. Roos, D. Brinkmann, K. Conder, and M. Eremin, *Phys. Rev. Lett.* **81**, 5912 (1998).

⁵D. Rubio Temprano, J. Mesot, S. Janssen, K. Conder, A. Furrer, H. Mutka, and K.A. Mller, *Phys. Rev. Lett.* **84**, 1990 (2000).

⁶M. d’Astuto, P.K. Mang, P. Giura, A. Shukla, P. Ghigna, A. Mirone, M. Braden, M. Greven, M. Krisch, and F. Sette, *Phys. Rev. Lett.* **88**, 167002 (2002).

⁷B. Friedl, C. Thomsen, and M. Cardona, *Phys. Rev. Lett.* **65**, 915 (1990).

⁸A. Lanzara, P.V. Bogdanov, X.J. Zhou, S.A. Kellar, D.L. Feng,

E.D. Lu, T. Yoshida, H. Eisaki, A. Fujimori, J.-I. Shimoyama, T. Noda, S. Uchida, Z. Hussain, and Z.-X. Shen, *Nature (London)* **412**, 510 (2001).

⁹M.L. Kulić, *Phys. Rep.* **338**, 1 (2000).

¹⁰R. Zeyher and M.L. Kulić, *Phys. Rev. B* **53**, 2850 (1996).

¹¹M. Grilli and C. Castellani, *Phys. Rev. B* **50**, 16880 (1994).

¹²Z.B. Huang, W. Hanke, E. Arrigoni, and D.J. Scalapino, *cond-mat/030613* (unpublished).

¹³M. Weger, M. Peter, and L.P. Pitaevskii, *Z. Phys. B: Condens. Matter* **101**, 573 (1996).

¹⁴D. Fay and M. Weger, *Phys. Rev. B* **62**, 15 208 (2000).

¹⁵A.A. Abrikosov, *Physica C* **222**, 191 (1994).

¹⁶R. Chitra and G. Kotliar, *Phys. Rev. Lett.* **84**, 3678 (2000).

¹⁷L. Pietronero, S. Strässler, and C. Grimaldi, *Phys. Rev. B* **52**, 10 516 (1995).

¹⁸C. Grimaldi, L. Pietronero, and S. Strässler, *Phys. Rev. B* **52**,

- 10 530 (1995).
- ¹⁹C. Grimaldi, L. Pietronero, and S. Strässler, Phys. Rev. Lett. **75**, 1158 (1995).
- ²⁰A.B. Migdal, Zh. Éksp. Teor. Fiz. **34**, 1438 (1958) [Sov. Phys. JETP **7**, 996 (1958)].
- ²¹A.I. Liechtenstein and M.L. Kulić, Physica C **245**, 186 (1995).
- ²²A.A. Abrikosov, Physica C **214**, 107 (1993).
- ²³J. Bouvier and J. Bok, Physica C **249**, 117 (1995).
- ²⁴I. Chang, J. Friedel, and M. Kohmoto, Europhys. Lett. **50**, 782 (2000).
- ²⁵P. Paci, C. Grimaldi, and L. Pietronero, Eur. Phys. J. B **17**, 235 (2000).
- ²⁶A. A. Abrikosov, L. P. Gorkov, and I. E. Dzyaloshinski, *Methods of Quantum Field Theory in Statistical Physics* (Dover, New York, 1963).
- ²⁷For a review: *Correlated Electron Systems*, edited by V. J. Emery (World Scientific, Singapore, 1993).
- ²⁸J. Hubbard, Proc. R. Soc. London, Ser. A **276**, 238 (1963).
- ²⁹M.C. Gutzwiller, Phys. Rev. Lett. **10**, 159 (1963).
- ³⁰G. Kotliar and A.E. Ruckenstein, Phys. Rev. Lett. **57**, 1362 (1986).
- ³¹A. Georges, G. Kotliar, W. Krauth, and M.J. Rozenberg, Rev. Mod. Phys. **68**, 13 (1996).
- ³²P. B. Allen and B. Mitrović, in *Solid State Physics*, edited by H. Ehrenreich, D. Turnbull, and F. Seitz (Academic, New York, 1982), Vol. 37.
- ³³G. D. Mahan, *Many-Particle Physics*, 3rd ed. (Kluwer Academic, New York, 2000).
- ³⁴W.E. Pickett, Rev. Mod. Phys. **61**, 433 (1989).
- ³⁵G. Baym and L. Kadanoff, Phys. Rev. **124**, 287 (1961).
- ³⁶M. Scattoni, C. Grimaldi, and L. Pietronero, Europhys. Lett. **47**, 588 (1999).
- ³⁷E. Cappelluti, C. Grimaldi, and L. Pietronero, Phys. Rev. B **64**, 125104 (2001).
- ³⁸H. Suhl *et al.*, Phys. Rev. Lett. **3**, 552 (1959).
- ³⁹A.Y. Liu, I.I. Mazin, and J. Kortus, Phys. Rev. Lett. **87**, 087005 (2001).
- ⁴⁰M.S. Osofsky, R.J. Soulen, Jr., J.H. Classen, G. Trotter, H. Kim, and J. Horwitz, Phys. Rev. B **66**, 020502 (2002).
- ⁴¹M.S. Osofsky, R.J. Soulen, Jr., J.H. Classen, G. Trotter, H. Kim, and J. Horwitz, Phys. Rev. Lett. **87**, 197004 (2001).